In situ measured current structures of the eddy field in the Mozambique Channel

5 authors, including:

Some of the authors of this publication are also working on these related projects:

Project — Ocean data assimilation in support of marine research and operational oceanography in South Africa
View project

Project — Western Indian Ocean Upwelling Research Initiative (WIOURI), part of the Second International Indian Ocean Expedition (IIO2) View project

In situ measured current structures of the eddy field in the Mozambique Channel

J.F. Ternon [a,*], M.J. Roberts [b,f], T. Morris [c], L. Hancke [c], B. Backeberg [d,e]

[a] Institut de Recherche pour le Développement, UMR 212 EME, 16 rue Claude Chappe, 97420 Le Port, La Réunion, France
[b] Oceans & Coasts Research, Department of Environmental Affairs, PO Box 52126, Victoria & Alfred Waterfront, Cape Town 8000, South Africa
[c] Bayworld Centre for Research and Education, PO Box 7296, Roggebaai 8012, Cape Town, South Africa
[d] Nansen-Tutu Centre for arine Environmental Research, Marine Research Institute, University of Cape Town, Rondebosch 7701, South Africa
[e] Nansen Environmental and Remote Sensing Center, Bergen, Norway
[f] Rhodes University, Grahamstown 6140, South Africa

ABSTRACT

Circulation and the related biological production have been studied during five cruises conducted in the Mozambique Channel (MZC) between 2005 and 2010. The circulation in the MZC is known to be highly turbulent, favouring enhanced primary production as a result of mesoscale eddy dynamics, and connectivity throughout the Channel due to the variable currents associated with migrating eddies. This paper presents the results of in situ measurements that characterize the horizontal and vertical currents in the surface and subsurface layers (0–500 m). The in situ data were analysed together with the geostrophic eddy field observed from satellite altimeter measurements. Different circulation regimes were investigated, including the "classical" anticyclonic eddy generated at the Channel narrows (16°S), the enhancement of southward migrating eddies by merging with structures (both cyclonic and anticyclonic) formed in the east of the Channel, and the presence of a fully developed cyclonic eddy at the Channel narrows. Comparison between in situ measurements (S-ADCP and velocities derived from surface drifters) and the geostrophic current derived from sea surface height measurements indicated that the latter can provide a reliable, quantitative description of eddy driven circulation in the MZC, with the exception that these currents are weaker by as much 30%. It is also suggested from in situ observation (drifters) that the departure from geostrophy of the surface circulation might be linked to strong wind conditions. Finally, our observations highlight that a-geostrophic currents need to be considered in future research to facilitate a more comprehensive description of the circulation in this area.

© 2013 Elsevier Ltd. All rights reserved.

1. Introduction

Due to its location between Madagascar and the coast of Africa, the ocean circulation in the Mozambique Channel (MZC) is turbulent and complex (Penven et al., 2006). The contribution of the southward flow through the MZC to the Agulhas Current system (Biastoch et al., 1999; Beal et al., 2011) makes the understanding of its source, nature and variability of major interest. Extensive reviews of research conducted since the 1950s have been outlined in Di Marco et al. (2002), Schouten et al. (2003), and Lutjeharms (2006), and have highlighted important questions such as the permanent presence of a southward flow along the African coast (i.e. the Mozambique Current—MC) and the sources of variability observed at seasonal or inter-annual scales.

Initially, analysis of ship drift data (e.g. Saerte, 1985; Lutjeharms et al., 2000) and data from hydrographic cruises (e.g. Saerte and Jorge da Silva (1984); Donguy and Piton, 1991) suggested that a southward flow along the African coast did indeed exist. However, its persistence throughout the year could not be demonstrated. It has long been suspected that the seasonality of the MZC circulation is linked to the South Asian Monsoon system, at least in the northern part of the Channel. Saerte and Jorge da Silva (1984) proposed two different circulation patterns corresponding respectively to the southern hemisphere summer (northeast monsoon, from November to April) and winter (southwest monsoon, May–October) (Fig. 1). A remarkable feature of their circulation scheme was the presence of rotating cells, both in the northern and southern part of the Channel. They identified three anticyclonic gyres as major components of the circulation, two of them merging in winter. Interestingly, Harris (1972) had already proposed a similar scheme from ship drift analysis, but with eddies of varying sizes and at different locations. Saerte and Jorge da Silva (1984) mentioned cyclonic cells of smaller size

* Corresponding author.
E-mail address: jean-francois.ternon@ird.fr (J.F. Ternon).
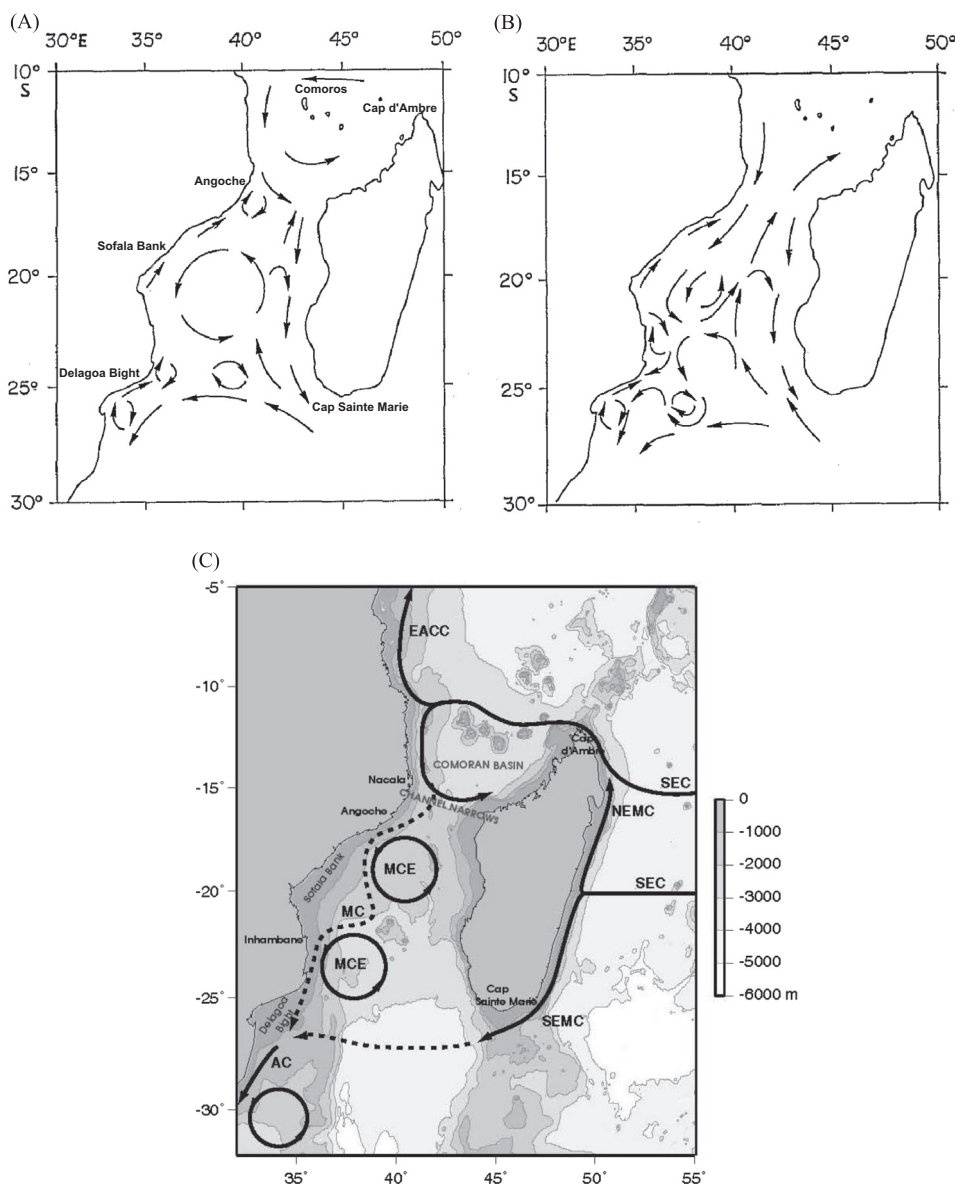
Fig. 1. Historical perspective of the circulation in the MZC, from Saerte and Jorge da Silva (1984) who proposed two schemes depending on the monsoon season: (A) northeast monsoon in austral summer, (B) southwest monsoon in austral winter, and (C) from Schouten et al. (2003), in a scheme dominated by the MZC eddies (MCE). Other currents include the South Equatorial Current (SEC), South East Madagascar Current (SEMC), North East Madagascar Current (NEMC), East African Coastal Current (EACC), and Agulhas Current (AC). Dotted lines stand for the uncertain Mozambique Current (MC) and for the unclear connection between the SEMC and AC. Geographic locations cited in the text are labelled. Bathymetry in (C) is featured in grey scale on the right.

within the Channel, some of them being quasi permanent (Fig. 1). They also depicted a northeastly coastal flow along the Sofala Bank for both seasons (Fig. 1). Accordingly, the semi-permanent cyclonic circulation near Angoche at 15°S (Lutjeharms, 2006) and in the Delagoa Bight (Quartly and Srokosz, 2004) appears to lead to a northward coastal flow. Donguy and Piton (1991), from the analysis of tide gauge records and hydrographic data, described a persistent anticyclonic gyre in the Comoran Basin (Fig. 1C), with seasonal and inter-annual variability in its intensity. However, they found that a strong southly flow exists across the narrows at ~16°S within the 0–500 m upper layer.

Mesoscale eddies have also been identified in the southern MZC, using surface drifter and hydrographic data. Gründlingh (1989) hypothesised that these features form locally near Madagascar and propagate westward, eventually reaching the Agulhas Current system (de Ruijter et al., 2004). Few observations have focused on the eastern side of the MZC. According to the circulation schemes of Saerte and Jorge da Silva (1984), the mean flow in

the eastern MZC is southerly (Fig. 1) but Saerte (1985) indicated that the few observations available make this result questionable.

Modern cruises with high precision CTD and S-ADCP (Ship borne-Acoustic Doppler Current Profiler) instrumentation, as well as drifter deployments, have been conducted in this region since the mid-1990s (e.g. Di Marco et al., 2002; Chapman et al., 2003; De Ruijter et al., 2004; Swart et al., 2010). These technologies have allowed for a better description of the MZC circulation and confirmed that (1) the circulation in the MZC is highly variable and eddy driven, and (2) the variability of this circulation is remotely constrained by the basin-scale variability within the Indian Ocean. Moreover, the mesoscale dynamics in the Channel are forced by the South Equatorial Current (SEC) that splits upon reaching the east coast of Madagascar at ~12°S: The northern branch (North Madagascar Current—NMC) flows towards the equator and past the northern tip of Madagascar (Cap d'Ambre, 12°S) while the East Madagascar Current (EMC) flows south towards Cape Ste Marie (25°S) at the southern tip of Madagascar

(e.g. Schouten et al., 2003; Fig. 1C). After passing Cap d'Ambre, the NMC flows westward and upon reaching the African coast, splits into a northerly branch (East African Coastal Current—EACC) and a southerly branch that flows into the northern MZC. This flow through the Channel narrows was thought to become the Mozambique Current (MC). From the trajectories of subsurface (900 m) ALACE floats, Di Marco et al. (2002) argued that, due to the presence of the Comoro Islands, the flow at intermediate depths originating from the northern latitudes circulates eastward rather than entering directly into the northern part of the Channel. Indeed, northern waters at intermediate depths join the westward NMC flow and enter the MZC after passing Cap d'Ambre at 12°S (Di Marco et al., 2002). Similarly, in the south, the EMC flows westwards after passing Cap Sainte Marie and plays a significant role in the formation of eddies (or pairs of eddies) near the southern tip of Madagascar which then drift westward or south-westward until they eventually reach the Agulhas Current (de Ruijter et al., 2004; Quartly and Srokosz, 2004).

Remote sensed altimetry has greatly improved our understanding of the circulation in the MZC. Schouten et al. (2003) tracked 25 anticyclonic eddies between 1995 and 2000, and showed that these features propagated preferentially to the south along the coast of Mozambique, with a frequency varying from seven eddies per year in the north to four per year in the south. The SSH anomaly of these eddies was shown to vary along their trajectory, with maximum eddy amplitude being reached in the middle of the Channel at 20–24°S. Quartly and Srokosz (2004) successfully used ocean colour from SeaWiFS (1998–2003) to distinguish cyclonic and anticyclonic eddies moving from Cap Sainte Marie along the west coast of Madagascar to 23°S.

An array of current-metres deployed in 2000 to depths of 2000 m across the narrows of the Channel at ~16°S allowed for a long term study of the flow through the MZC (De Ruijter et al., 2002; Ridderinkhof and De Ruijter, 2003). Using data recorded during the first 2 years of measurement (2001–2002), Ridderinkhof and De Ruijter (2003) showed that there is no continuous MC along the coast of Mozambique, but rather strong current events occur on the western side of the mooring array, corresponding to the passage of anticyclonic eddies. These eddies occur at a frequency of nine events over a 2 year period, compatible with that proposed by Schouten et al. (2003). The net flow across the Channel narrows was found to be southerly throughout the year. The eddies crossing the mooring array were shown to be essentially barotropic, with both the southerly and northerly flow component of the eddy extending down to 2000 m (Ridderinkhof and De Ruijter, 2003). The current metre array was re-deployed in 2003 and has been regularly serviced since then (LOCO programme, De Ruijter et al., 2006).

A robust cyclic mechanism for the generation of anticyclonic eddies at the Channel narrows has been proposed by Harlander et al. (2009). The start of the cycle is associated with the appearance of a strong southerly current at the eastern edge of the mooring array. Once generated, eddies interact with anticyclonic structures from the east of the Channel (Palastanga et al., 2006). These control the growth of the eddy during its southward displacement along the Mozambican coast. In contrast, interaction

with a cyclonic structure results in the decay of the eddy during its displacement. The authors related the resulting variability in the eddy field to the large scale variability in the Indian Ocean basin, especially the Indian Ocean Dipole (IOD, Saji et al., 1999). A positive IOD index has been related to a decrease in the strength of the SEC and to a subsequent decrease of the southerly transport through the Channel narrows in the MZC. Conversely, a negative IOD index has been shown to correspond to an increased southerly transport. This occurs with a time lag of about 1 year (Ridderinkhof et al., 2010). Harlander et al. (2009) proposed that internal Rossby normal modes could be triggered by the large scale oscillations and be the local control of eddy dynamic variability.

Advances in modelling have also contributed to understanding spatial and temporal variability of the circulation in the MZC. In particular, analyses of model outputs have suggested possible mechanisms for the generation of eddies (Biastoch and Krauss, 1999; Backeberg and Reason, 2010) and their distribution and evolution within the MZC (Halo et al., 2014). These model studies similarly indicate that the eddy turbulence in the MZC is driven by remote, basin-scale, forces as suggested by the in situ observation.

We present new current data obtained during research cruises in different sectors and at different seasons in the MZC between 2005 and 2010. Ocean current estimates were derived from S-ADCP measurements along the ship track. Near surface circulation was interpreted together with Sea Level Anomaly (SLA) data and surface drifters deployed during the cruises (Hancke et al., 2014). Circulation patterns are presented with emphasis on both the horizontal and vertical components. In situ observations are compared to the current field observed from satellite altimetry, and the potential importance of the a-geostrophic circulation (including an Ekman component) in the MZC is assessed.

2. Data and methods

2.1. Current measurements

Underway current profiles (S-ADCP) were measured using three different ships over a number of cruises (Table 1). A 75 kHz RDI Ocean Surveyor II with a time average of 3 min per ensemble was used on cruises MC05 and MC07, while a 150 kHz RDI Ocean Surveyor I with a time average of 3 min per ensemble was used on cruise MC08A. A 75 kHz RDI Ocean Surveyor II using a time average of 2 min was utilised on cruise MC10A. The entire S-ADCP data set was processed using the CASCADE software (released by IFREMER, France) which allows "flagging" of the data according to statistical and threshold analysis, as well as horizontal and vertical filtering. Standard settings included (1) a reference layer for profile validation selected between cells 3 and 5 (e.g. 16–48 m), (2) a maximum horizontal velocity set at 200 cm s^{-1}, and (3) an error threshold on the vertical velocity set at 10 cm s^{-1}. Vertical profiles extended to between 300 m and 500 m depending on the frequency of the instrument used. Finally, the profiles were averaged over 5 km (1/12°) intervals for plotting and further calculation. Data taken during the stations (no ship motion) were

Table 1
Current measurements during the five cruises.

Year	Code	Cruise name	Ship	Date	S-ADCP	L-ADCP	Drifters
2005	MC05	ACEP 2005	R.V. *Algoa*	04-08-05/05-02-05	Yes	No	Yes
2007	MC07	ACEP 2007	R.V. *Algoa*	09-10-07/09-23-07	Yes	No	Yes
2008	MC08A	ASCLME 2008	R.V. *Fridtjof Nansen*	11-28-08/12-17-08	Yes	No	Yes
2009	MC09B	MESOP 2009	R.V. *Antea*	10-27-09/11-24-09	No	Yes	Yes
2010	MC10A	MESOP 2010	R.V. *Antea*	04-07-10/05-08-10	Yes	Yes	No

discarded. No specific tidal correction was applied to the data set as the main focus of the study was on structures characterized by strong geostrophic currents (~ 1 m s^{-1}) and tidal noise lower than 4–7 cm s^{-1} have been reported in the study area (Di Marco et al., 2002), except at specific locations: 0.1 m s^{-1} at Cape Amber (Di Marco et al., 2002); internal tide on the Sofala Bank (Manders et al., 2004; Da Silva et al., 2009).

2.2. Surface drifters

Twenty-two satellite tracked surface drifters (drogued at a depth of 10 m) were deployed in the Channel during research cruises between 2004 and 2009, either on the edge, or near the centre of the selected eddies (details in Hancke et al., 2014). The u and ν components of velocity for each drifter were calculated from the 6-hourly position reports. Daily averaged velocities were calculated and attributed to the mid-point (median) position for that day. In addition, data for 60 drifters from the Global Drifter Program (GDP; http://www.aoml.noaa.gov/phod/dac/) tracked in the Mozambique Channel between 2000 and 2010 were also used (Hancke et al., 2014). The GDP data included both u and ν components and the magnitude of the velocity at 6-hourly intervals. The same methodology was applied to calculate daily mean velocity at the mid-position for that day and for each drifter. Error of the drifting buoy-derived velocities is a combination of the slippage of the drifter due to the effect of wind and waves (less than 1 cm s^{-1} in winds of 10 m s^{-1}, Niiler et al., 1995) and the accuracy of the location of the drifter estimated for a 6-h trajectory (corresponding to a precision of ~ 5 cm s^{-1}, Thomson et al., 1998). This corresponded to an overall error of the drifting buoy-derived velocity of ~ 7 cm s^{-1} (Uchida et al., 1998).

2.3. Altimetry data

To describe the MZC eddy field for the period of the cruises, we used the weekly "Updated Delayed Time" (DT) mapped Sea Level Anomaly (MSLA) gridded at 1/3° resolution, produced by Ssalto/Duacs and distributed by AVISO and CNES (http://ftp.aviso.oceanobs.com/duacs/). The Sea Level Anomaly (SLA) was chosen as it is better suited for the identification of transient mesoscale features. The merged, multi-satellite products were used which provided improved accuracy for studies of mesoscale variability (Le Traon and Dibarboure, 1999; Ducet et al., 2000; Pascual et al., 2006).

For the quantitative comparison between (altimetry-derived) geostrophic velocity, S-ADCP velocities, and the velocities derived from surface drifters, the absolute dynamic topography (MADT) was used instead of SLA. The DT (delayed time) daily MADT product, with a horizontal resolution of 1/3°, was utilised. This product combines sea level anomaly observations with the Rio09 mean dynamic topography (Rio et al., 2011), using data from up to four satellites at a given time.

2.4. Wind data and Ekman surface current

The Mean Wind Field (MWF) wind data was downloaded for 2003–2009, corresponding to the period of drifter deployments. This is a daily product with a spatial resolution of 1/2° (55 km) from the QuikSCAT/SEAWINDS scatterometer (http://podaac.jpl.nasa.gov),

which is distributed by CERSAT (Centre for Satellite Exploitation and Research)/IFREMER. Since QuikSCAT failed in November 2009, wind data for 2010 was obtained from the Advanced Scatterometer (METOP-A/ASCAT) as a daily product with a spatial resolution of a 1/4°. Only QuikSCAT data was used to calculate the Ekman component of the surface circulation for comparison with the altimetry-derived geostrophic velocity and drifter velocity. The Ekman surface current was calculated using the satellite wind speed at a height of 10 m following the classical method of Stewart (2004).

A global analysis of the wind field was also performed over a grid of the MZC, composed of four latitudinal bands (4° width) divided in zones of about 4° longitude (Table 2). Within each of the 10 zones, the percentage of wind speed within speed classes (0–4 m s^{-1}, 4–8 m s^{-1}, 8–12 m s^{-1}, 12–16 m s^{-1}, 16–20 m s^{-1}) was calculated on a yearly basis for the 8 years of satellite wind data (2003–2010). A mean distribution of the yearly mean wind speed classification was estimated for the whole period (2003–2010). The same analysis was performed for periods corresponding to the peak influence of both the northeast and southwest monsoon (November–February, May–September respectively) in order to investigate the monsoon influence over the whole MZC (wind speed and direction). An empirical relationship was used to estimate the corresponding Ekman current speed classes (Pond and Pickard, 1983):

$$V_0 = W * \frac{0.0127}{(\sin |\Phi|)^{1/2}} \tag{1}$$

where V_0 is the Ekman surface current speed (m s^{-1}), W is the wind speed (m s^{-1}) and Φ is latitude (20°S for our estimate).

2.5. Altimetry versus in situ velocity comparison (ADCP and drifter derived)

The comparison was done using the S-ADCP data for cruises MC07 and MC08A. For the S-ADCP-altimetry comparison, longitude, latitude and the corresponding u and ν components of the in situ velocity were extracted at 5 km resolution. No daily mean was calculated for the S-ADCP velocity as the ship might have crossed an entire eddy within 1 day. Instead, altimetry data was interpolated to all the S-ADCP positions for each successive day. The interpolation was done using the "nearest neighbour" method (e.g. Murat Yilmaz, 2007).

A linear relation was assessed for in situ (ADCP) velocities and those estimated from altimetry. From a statistical point of view, the approach suffered from (1) the non-normal distribution of the current data (a gamma distribution was a better fit) and (2) the autocorrelation between successive measurements. A bootstrap procedure (Davison and Hinkley, 1997), with a 1/35 sub-sampling rate and $N=3000$ iterations, enabled the autocorrelation to be cleared and also provided an error estimate for the parameters of the linear model.

For the drifter-altimetry-velocity comparison, the daily mean position and u and ν components for each drifter were determined. Altimetry data for each corresponding date was interpolated to the mean drifter position using the "nearest neighbour" method.

Table 2
Latitude–longitude limits of the 10 boxes of the gridding used for the wind speed analysis.

	Zone 1	Zone 2	Zone 3	Zone 4	Zone 5	Zone 6	Zone 7	Zone 8	Zone 9	Zone 10
Latitude	12–16°S	12–16°S	16–20°S	16–20°S	20–24°S	20–24°S	24–28°S	24–28°S	24–28°S	24–28°S
Longitude	40–44°E	44–48°E	34–40°E	40–46°E	34–40°E	40–45°E	32–36°E	36–40°E	40–44°E	44–48°E
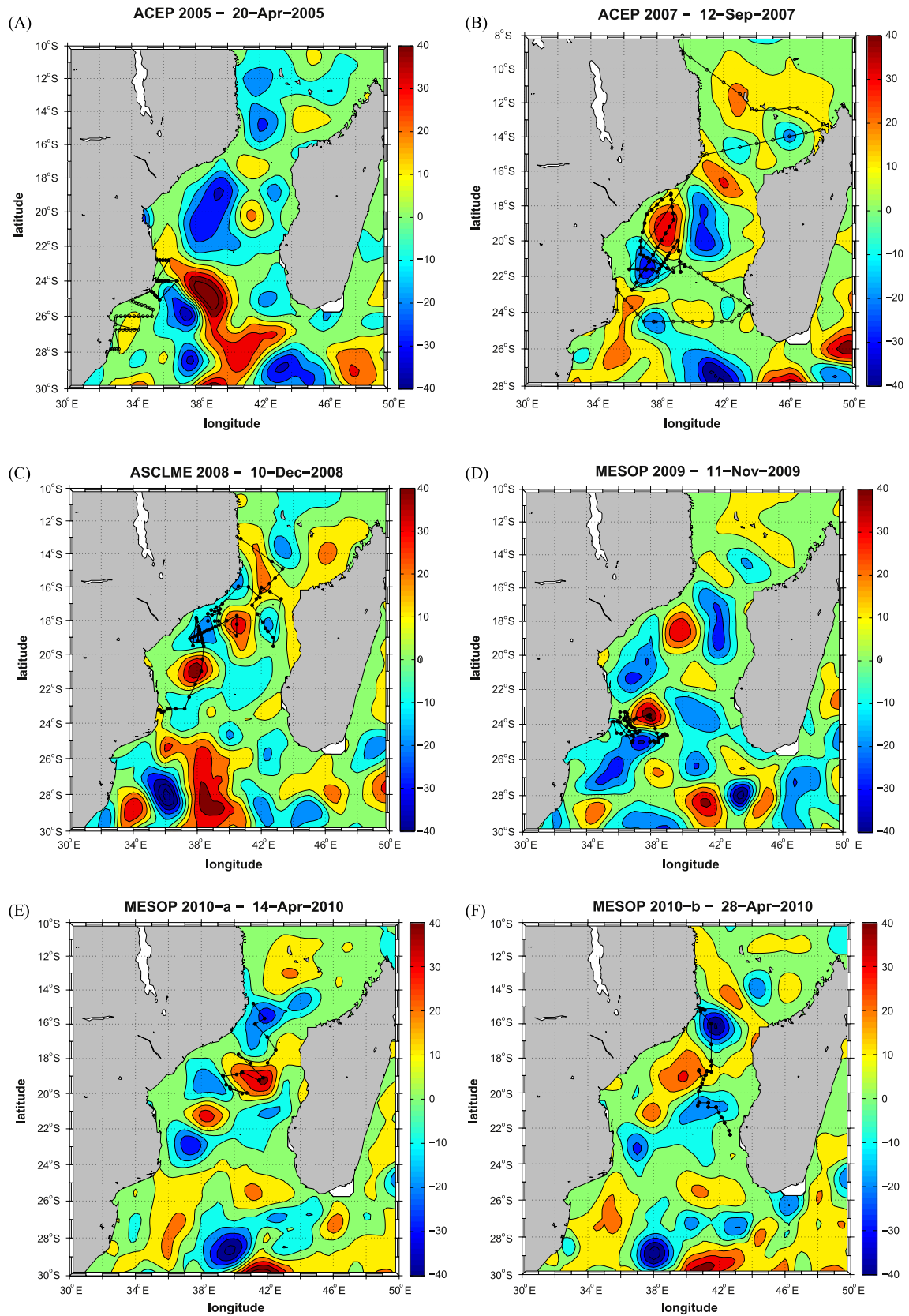
Fig. 2. Maps of cruise tracks conducted between 2005 and 2010 in the MZC superimposed on the eddy field for a given day during the cruise. Black dots and open circles represent hydrographic stations.

2.6. Ekman velocity versus altimetry geostrophic current

Daily wind and altimetry products were used for the comparison between geostrophic and wind driven surface velocities in the MZC. Interpolation ("nearest neighbour" method) was used to match the altimetry data (1/3°) to each wind data location (1/2° resolution).

The comparison between geostrophy, wind and drifter velocities was performed at the daily mean position of the drifters for the period 2003–2009 (QuikSCAT/SEAWINDS data set). Interpolation of the Ekman surface current, calculated from QuikSCAT wind data, to the daily drifter position was also performed using the nearest neighbour method. For each position, in situ surface velocities (drifter), geostrophic (altimetry) and Ekman (wind data) components of the velocity were obtained.

2.7. Field sampling strategy

Five multidisciplinary cruises were undertaken during 2005–2010 (Fig. 2), covering an area that ranged from the Channel narrows (14°S) to Delagoa Bight (26°S) (Fig. 1C). The western and central MZC were surveyed more intensively, with the exception of the 2010 cruise where some stations were occupied between 20° and 23°S. Cross Channel transects were undertaken in the southern and northern regions of the MZC in 2007. Along track S-ADCP data was recorded during all cruises except for 2009 (only lowered L-ADCP was available for this cruise).

Where possible the cruises targeted well defined dipoles (2005, 2007, 2009) or surveyed a more extensive eddy field comprising several cyclones and anticyclones (2008, 2010). In 2008, the ship track successively sampled a weak cyclone in the northern basin, a newly formed anticyclone in the Channel narrows (16°S), and then cyclones and anticyclones located along the western side of the MZC to 23°S. In 2010, an anticyclone was first investigated in the centre of the Channel before it rapidly shifted southwestwards halfway through the cruise, then a cyclonic feature located roughly at the latitude of the narrows (∼16°S) was studied, and finally eddies located in the east and southeast were surveyed. Convergence areas, to the west of eddy dipole structures, with an anticyclone to the north and a cyclone to the south, were examined in 2005, 2007, 2008 and 2009. Divergence areas, to the east of the above eddy dipole structures, were surveyed in 2007, 2008 and 2009. Cruise tracks directed right across dipoles were undertaken in 2007, 2008 and 2010.

3. Results

3.1. Wind conditions in the Mozambique Channel

Two seasons were investigated in this study, these being austral summer (September–December) and austral autumn (April–May). These seasons were not in phase with the monsoon but, at these latitudes, the monsoon influence is known to be weak (Saerte and Jorge da Silva, 1984; Lutjeharms, 2006) except in the north of the Channel (Bigg, 1992). According to Sete et al. (2002), northeast winds dominate along the northern coast of Mozambique (e.g. Pemba, 13°S) in the austral summer (northeast monsoon) and southwest winds dominate during the austral winter (southwest monsoon). Along the central and southern Mozambique coasts, southeast trades dominate all year long, the southerly winds being guided locally by the shape of the Channel (Bigg, 1992).

The satellite wind data are in agreement with these general trends. The analysis of the 2003–2010 time series in the sectors previously defined (Table 2, Fig. 11A) clearly highlighted (1) the repeatability of the trends in each sector from year to year (Fig. 11B, error bars), (2) the occurrence of the northeast monsoon

winds in the northern zones 1–4 only, mainly from November to February, (3) the generally higher wind speed south of 20°S, especially for wind entering the Channel south of Madagascar (Fig. 11B, zones 9 and 10), and (4) the high variability in the direction of the westerlies reaching the coast of Mozambique (zone 7, measured during cruises MC07 and MC09B). Malauene et al. (2014) also noted the two wind regimes related to the monsoon winds offshore of Angoche (16°S), with the southwest winds being generally stronger than the northeast winds.

Superimposed on these seasonal trends, considerable short timescale variability (daily) in wind conditions were experienced during the research cruises, especially in the southwest sector of the study area. Episodes of winds stronger than 10 m s^{-1} (20 knots) occurred during the cruises in September 2007 and November 2009. Weak to moderate winds, with high daily variability, were experienced in November 2008 and April 2010.

3.2. Eddy field during MESOBIO

The eddy pair investigated off Inhambane in April 2005 (Fig. 2A) resulted from the merging of four anticyclones that were formed in the northern and eastern MZC several weeks before the cruise. The first anticyclone was tracked from November 2004 when it formed in the narrows before merging with three other anticyclones, two of which formed in the eastern MZC. The cyclonic component of the dipole remained closely associated with the anticyclone for two months prior to the cruise. In contrast to the 2005 dipole, the anticyclonic component of the dipole investigated in November 2009 (Fig. 2D) resulted from the merging of only two anticyclones originating from the northern MZC. This dipole formed about 2 months before the cruise commenced and drifted to the location of study by the beginning of the cruise and remained stable for the duration.

During the 2007 (Fig. 2B) and 2008 (Fig. 2D) surveys, the eddy field in the MZC consisted of suites of anticyclones formed in the northern basin and in the Channel narrows, and cyclones that evolved in response to the dynamics of the anticyclones. A cyclone that formed west of Madagascar in August 2007 developed along 40°E while the anticyclone investigated during the cruise shifted westward toward the Sofala Bank at 20°S (Fig. 1C). In 2008, an anticyclone formed west of Madagascar at 21°S and merged 2 months later with the anticyclone originating from the north that was studied at 39°E.

The eddy field in 2010 had two specific characteristics not seen in the previous eddy fields: (1) a strong eastern component as both an anticyclone and two cyclones were part of the features investigated during the cruise, and (2) the presence of a well developed cyclone at the latitude of the Channel narrows instead of the usually observed anticyclone at this location. This resulted in an atypical eddy pattern in early May 2010 (Fig. 2F) when the central MZC was dominated by a strong cyclone located between 15° and 18°S and a large anticylonic cell in the west between 17° and 22°S (and a weak cyclonic structure in the east of the basin at these latitudes).

It should be noted that prior to, or during most of the cruises (2007, 2008, 2009 and to a lesser extent in 2010), a small cyclonic cell was observed in the eastern sector of the northern MZC basin. This cyclone was studied (S-ADCP) in 2007 (Fig. 2B) when the ship sailed to Nosy-Be at the end of the cruise MC07. Such a feature was also suspected to be present during a cruise along the western coast of Madagascar in September 2009 (see Pripp et al., 2014).

3.3. In situ observation of the velocity field

3.3.1. Zonal transects across the MZC (September 2007)

A zonal transect across the southern Channel at 24.5°S from west to east is presented in Fig. 3. West of 40°E, satellite altimetry
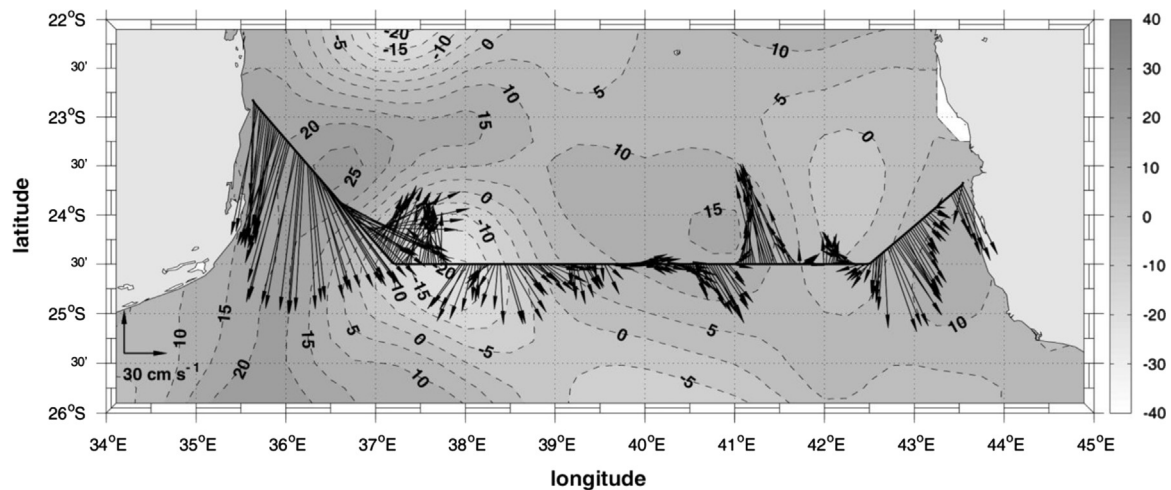
Fig. 3. Near surface (0–50 m) velocity in the southern Mozambique Channel measured during cruise MC07, superimposed on the eddy field for 12 September 2007. Grey scale indicates SLA (cm). A velocity scale is shown in the bottom left corner.

indicated that the cruise track crossed an anticyclone centred at 23.5°S, 36.5°E, then a cyclone centred at 24.5°S, 37.75°E. The anticyclone was associated with a strong southwesterly flow, with an ADCP mean speed up to 1.2 m s^{-1} in the 0–50 m surface layer. This current contributed to the southward flow along the Mozambique shelf. The cyclonic cell was also clearly evident in the ADCP data, with speeds up to 0.60 m s^{-1} at its edge. East of 40°E, ADCP measurements were consistent with an anticyclonic flow between 40.5°E and 41.5°E, and with a cyclonic cell associated with strong southeasterly flow at ~43°E. The currents along the section were most pronounced in the upper 200 m and remained apparent to depths of 600 m, which is also the maximum penetration depth of the ADCP. Of interest is a strong southeasterly coastal current (up to 0.50 m s^{-1}) evident at 23.5°–24°S off Madagascar, which remained independent of the southeasterly branch of the easternmost cyclone (Fig. 3).

A second transect across the northern Channel was undertaken between 15°S, 41.5°E (Mozambique) and 13.5°S, 47.5°S (Madagascar) (Fig. 4A, southern leg), transecting a dipole with the anticyclonic core centred at 14.5°S, 43°E and the cyclonic core at 14°S, 46°E. The surface (0–50 m) ADCP currents closely agreed with the position of the two eddies observed by satellite altimetry (Fig. 4A). Flow in the western sector contributed towards a general anticyclonic gyre circulation in the northern basin of the MZC (see northern transect, Fig. 4A). In the east, a consistent southeasterly current flowed between the edge of the cyclone and the coast of Madagascar. According to the altimetry, this cyclone remained stable in the northern basin from mid-July until early November 2007. Such a circulation pattern has also been observed during a cruise in September 2009 (Pripp et al., 2014). West of the anticyclone, southeasterly surface currents attained velocities up to 2.0 m s^{-1}, while those east of the cyclone reached 0.55 m s^{-1}. On the eastern side of the anticyclone, the northward current component was 1.1 m s^{-1}, with up to 0.75 m s^{-1} being observed on the western limb of the cyclone. These currents extended down to 600 m on the western boundary of the dipole and ~200 m elsewhere.

The third cross Channel transect spanned the northern MZC basin (Comoran Basin) between the Madagascar continental shelf (Nosy Be) and the African coast (southern Tanzania), north of the above mentioned dipole (Fig. 4A, northern leg) and transecting close to the islands of the Comoros archipelago. North of the Comoros, an elongated anticyclonic cell was fully developed with a SLA of > 20 cm. In this case, the surface currents (0–50 m) did not agree closely with the observations from satellite altimetry and seemed to be constrained by the islands of the Comoros

archipelago (Fig. 4B). The flow was predominantly southwesterly east of Grande Comore (43.25°E), suggesting an anticyclonic circulation in the Comoran Basin, complementing the observation above. Unfortunately, the transect was too far to the south to capture the westward flow passed the northern tip of Madagascar. However, the southwesterly flow east of Grande Comore may be part of this westward flow entering the northern MZC.

3.3.2. Dipole transects (September 2007 and December 2008)

Horizontal surface (0–50 m) currents measured by the S-ADCP across and around a dipole that was investigated in 2007 are shown in Fig. 5. The anticyclonic and cyclonic eddies had comparable SLA amplitudes of ~40 cm, and the anticyclone was larger than the cyclone with a southwest–northeast diameter of 280 km versus 170 km for the cyclone. Variations in the mean surface current velocity across the dipole clearly displayed evidence of stronger dynamics in the anticyclone compared to the cyclone (Fig. 5C). The velocities up to 1.60 m s^{-1} were measured on the western edge of the anticyclonic eddy not far from the Mozambique shelf edge. In contrast, the surface current was only 0.65 m s^{-1} on the western edge of the cyclone. Velocities of ~1.30 m s^{-1} were measured at the boundary between the two eddies.

The vertical pattern of the currents is illustrated in the dipole that was investigated during the December 2008 cruise at 18°–19°S and 37°–42°E (Fig. 6). Similar to 2007, the anticyclone was more developed than the cyclone, where the SLA in the cyclone was only −15 cm but was 30 cm in the anticyclone. Maximum surface velocity (1.75 m s^{-1}) was measured at the western edge of the anti-cyclone (Fig. 6A, C). At 150 m, velocity was still 1.00 m s^{-1} at the edge of the eddy (point A in Fig. 6A, B) while almost zero velocities were measured in the centre of the eddy. Maximum surface velocity at the boundary of the cyclone was < 0.50 m s^{-1}, and within the width of the current core velocity was limited to 0.25 m s^{-1} at 75 m depth (sections E–F). The end of the transect (point G) coincided with the edge of a neighbouring anticyclone to the south of the cyclone (Fig. 6A).

3.3.3. Central versus eastern MZC circulation (April 2010)

The eddy field during leg 1 of the MC10A cruise included a stable and well developed cyclonic eddy between 15°S and 17°S in the western part of the Channel narrows and a well-defined anticyclone at ~19°S (Fig. 7). The anticyclone rapidly propagated to the west 1 week later. A weak and elongated cyclonic structure
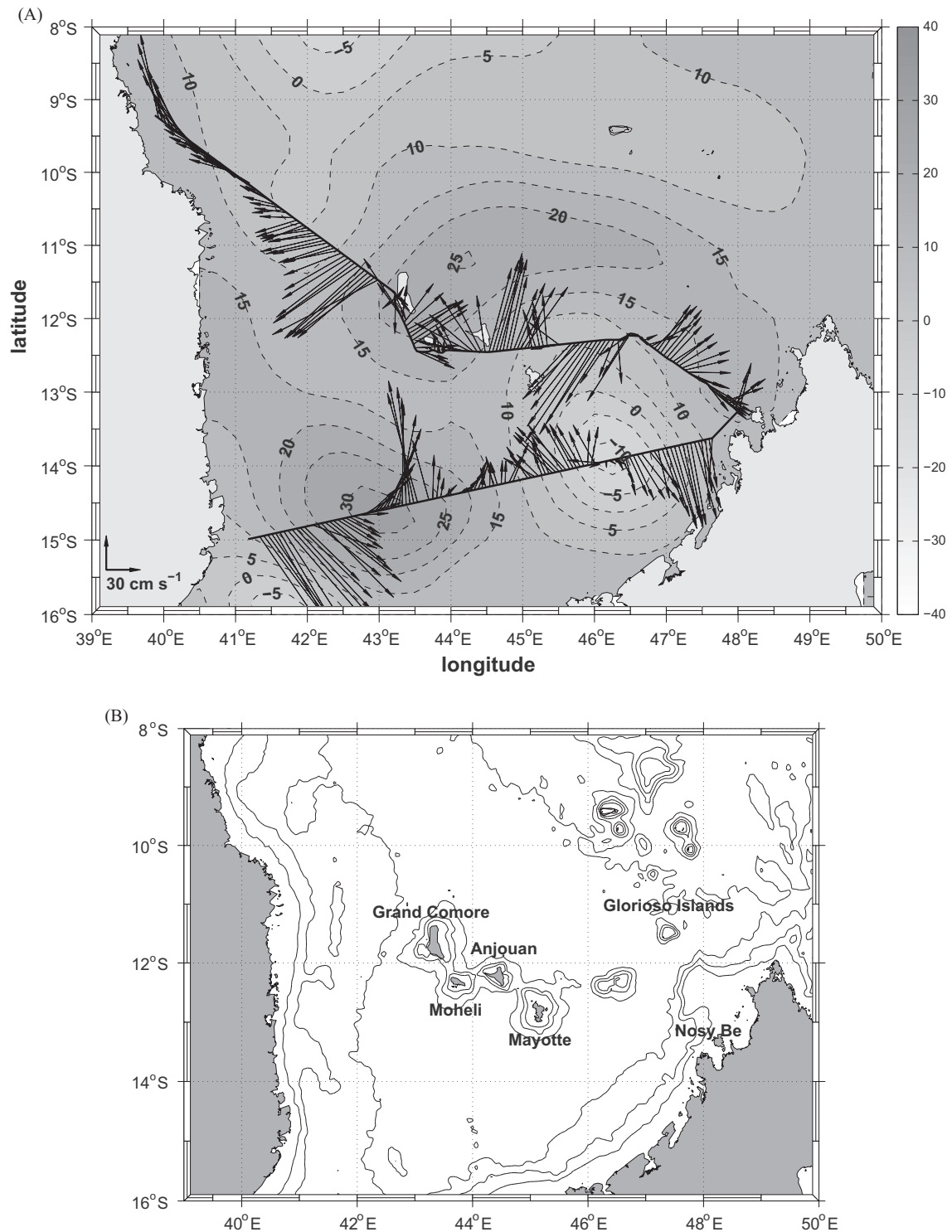
Fig. 4. Near surface circulation (0–50 m) in the Comoran basin (cruise MC07): (A) velocity field superimposed on the eddy field for 3 October 2007, and (B) bathymetry of the Comoran basin and locations cited in the text. Grey scale indicates SLA (cm). Velocity scale is shown in the bottom left corner. (Comoros archipelago: from Grande Comore in the west to the Glorioso Islands in the east. The Comoros include Grande Comore, Mohéli and Anjouan.)

($\sim$21°S) was investigated in the mid to eastern sector of the Channel at the end of leg 2 (Fig. 7C). Maximum velocities of 1.65 m s^{-1} (southeasterly current) were measured during leg 1 at the edge of the cyclone (point A in Fig. 7A). The eddy signature was clearly visible to depths of 300 m (maximum depth of the S-ADCP), with velocities up to 0.50 m s^{-1} to a depth of at least 200 m (points A and B in Fig. 7A, B and points H and I in Fig. 7C, D).

The velocity at the edge of the anticyclone (points D and F in Fig. 7A, B) attained 1.10 m s^{-1} at the surface during leg 1, with the eddy structure clearly visible to depths of 200 m.

Near the African continent, a coastal southwesterly current was evident during leg 2. This narrow current was opposite to the predominantly northeasterly flow at the edge of the cyclone (Fig. 8). Velocities up to 1 m s^{-1} were determined

(A)

(B)

(C)
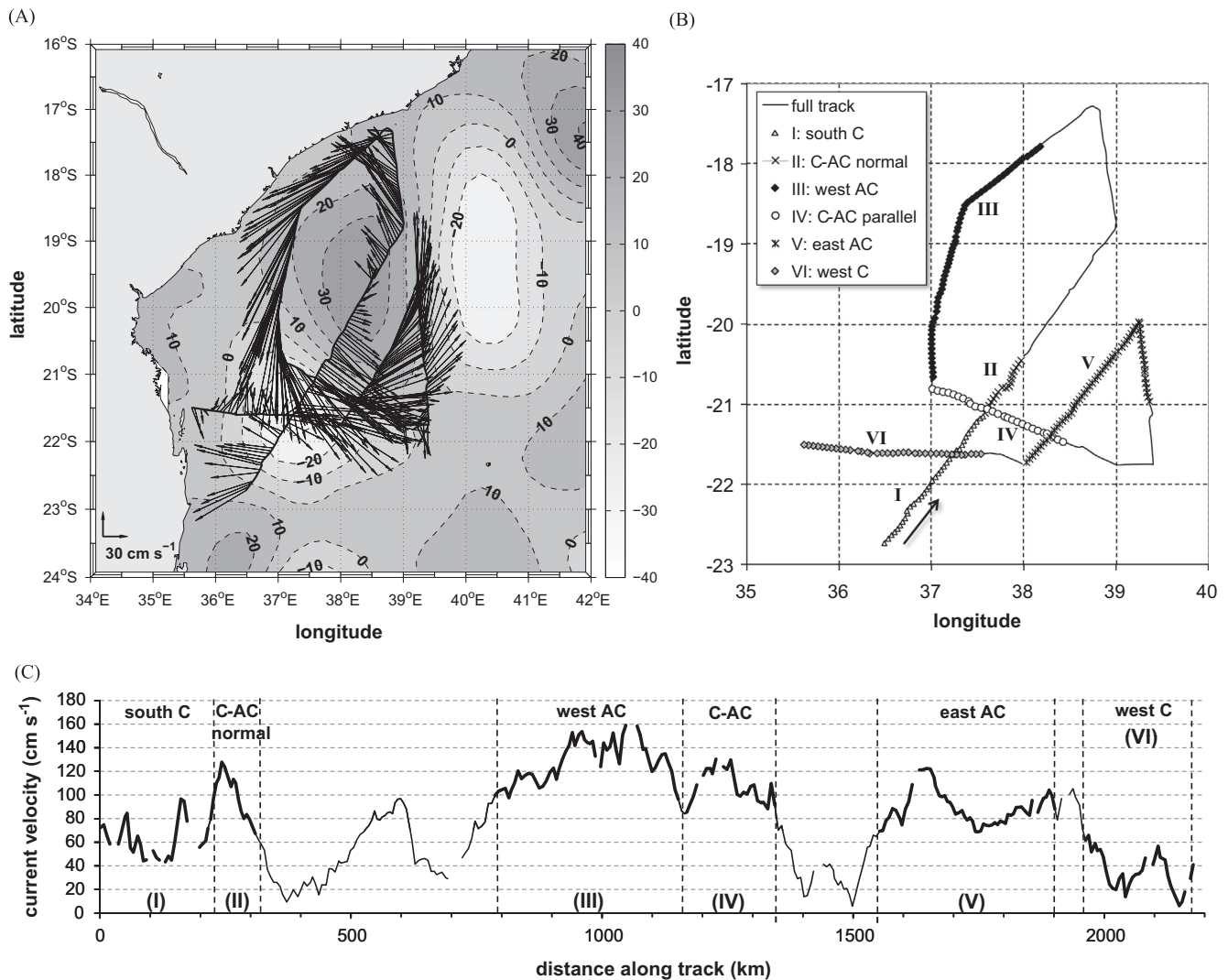
Fig. 5. Investigation of a dipole in the western Mozambique Channel (cruise MC07): (A) surface (0–50 m) velocity distribution over the eddy field for 19 September 2007, measured by an S-ADCP, (B) cruise track with the location of zones I–VI, and (C) magnitude of the surface (0–50 m) velocity along the cruise track (cm s^{-1}). within zones I–IV Grey scale indicates SLA (cm). Velocity scale (A) is shown in the bottom left corner.

within the core of this very narrow boundary current (20 km wide and 100 m deep). It should also be noted that a significant decrease in temperature was recorded during the same period by a UTR (Underwater Temperature Recorder) located at 18 m on Mozambique Island (http://www.cfoo.co.za/utr/utr.php?ID=118). The coastal current is consistent with the development of upwelling, resulting in lowered sea surface temperatures, as discussed by Malauene et al. (2014) for coastal upwelling in this area. As tide was not filtered out in the data sets, the influence of a tidal component in this flow pattern remains questionable. But Di Marco et al. (2002) and Manders et al. (2004) report a tidal component of < 10 cm s^{-1} near the surface in this area.

The circulation was much weaker south of 21°S. The southern most cyclone (20°–21.5°S) displayed velocities up to 0.45 cm s^{-1} and a limited vertical extent of ~ 100 m (depth of the 0.25 cm s^{-1} isoline, point K in Fig. 7B, F). Weak and reversing surface currents were measured along the southeast coast of Madagascar and it appeared that they were no longer structured by the eddy field. These observations suggest that the circulation in this area was not strongly associated with eddies, in agreement with the MC07 cruise data (zonal transect at 24.5°S, Section 3.3.1).

3.4. Comparison between in situ and remote observation of the velocity field

3.4.1. ADCP and SLA comparison

Comparison between along-track S-ADCP surface velocity and geostrophic velocity from altimetry is shown for two cruises (September 2007 and December 2008) in Fig. 9. Straight ship tracks favourable for such comparisons were selected. The relationship between ADCP measured currents and geostrophic velocities showed a similar trend for both cruises, despite a greater spread of data in 2007. This could be due to the steeper gradients in the sea surface topography observed during this cruise, corresponding to higher velocities (Fig. 9B) that were potentially smoothed by the low spatial resolution of the altimetry data set. The linear model explained only 40% of the variance ($R^2 = 0.413 \pm 0.154$) and the intercept (13.6 ± 10.5 cm s^{-1}) suggested an under-estimate of the surface velocity by the altimetry data. The poor correlation between both velocity data sets is mainly attributed to their very different resolution, namely the interpolated SLA derived geostrophic velocities *versus* instantaneous in situ measurements.

Correlation and biases between in situ and altimetry derived surface velocities have been estimated from large data sets of colocated measurements. Correlations up to 0.73 were found
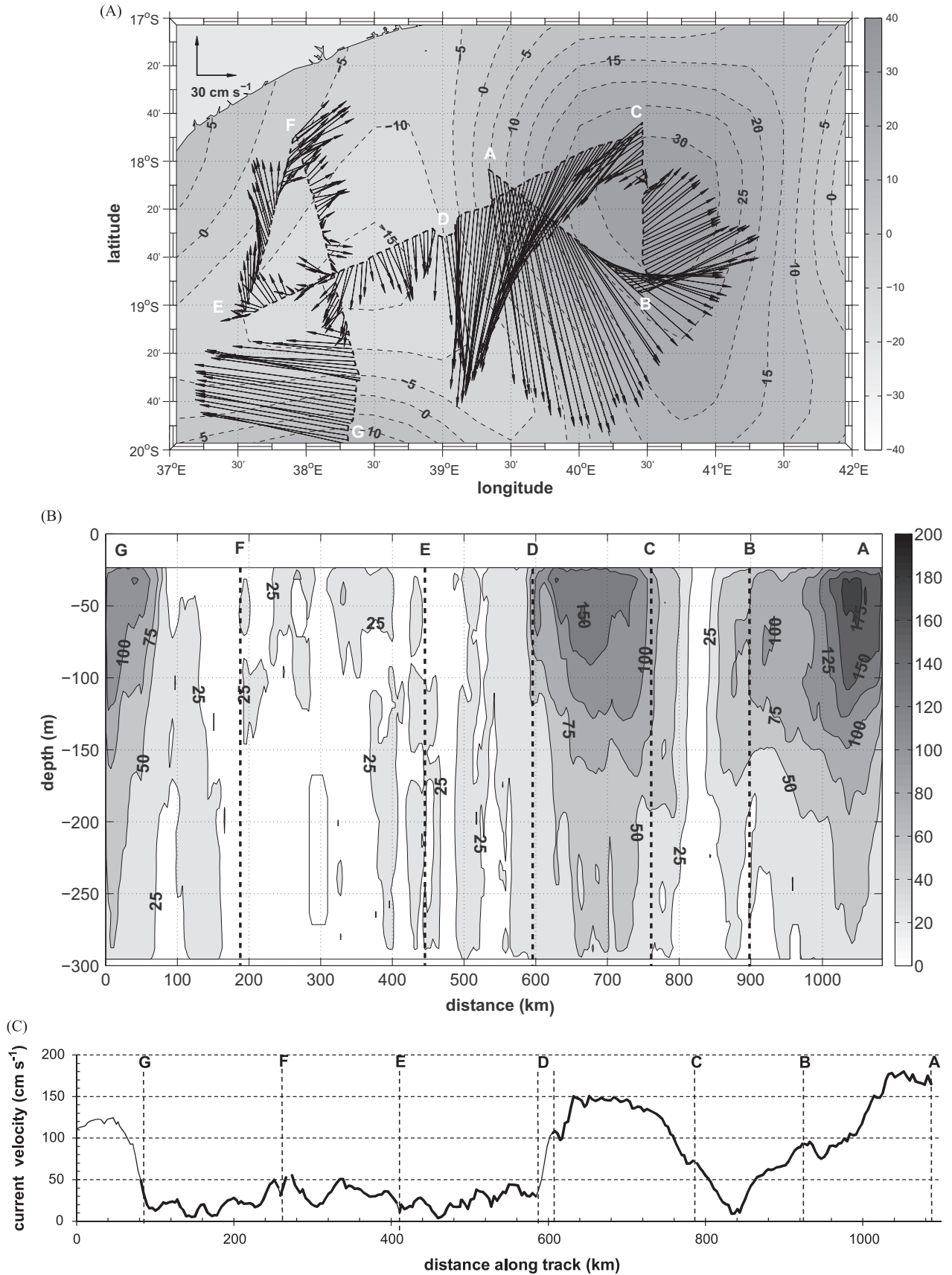
Fig. 6. S-ADCP measurements across an east–west dipole during the MC08 cruise: (A) surface velocity (0–50 m) over the eddy field for 10 December 2008, (B) vertical distribution of velocity (cm s^{-1}) along the transect A–G to a depth of 300 m, and (C) magnitude of the surface velocity (0–50 m) along the cruise track (cm s^{-1}). Grey scale indicates SLA (cm). Velocity scale (A) is shown in the top left corner. Heavy line in (C) corresponds to the data used for the mean eddy characteristics assessed in Table 3.
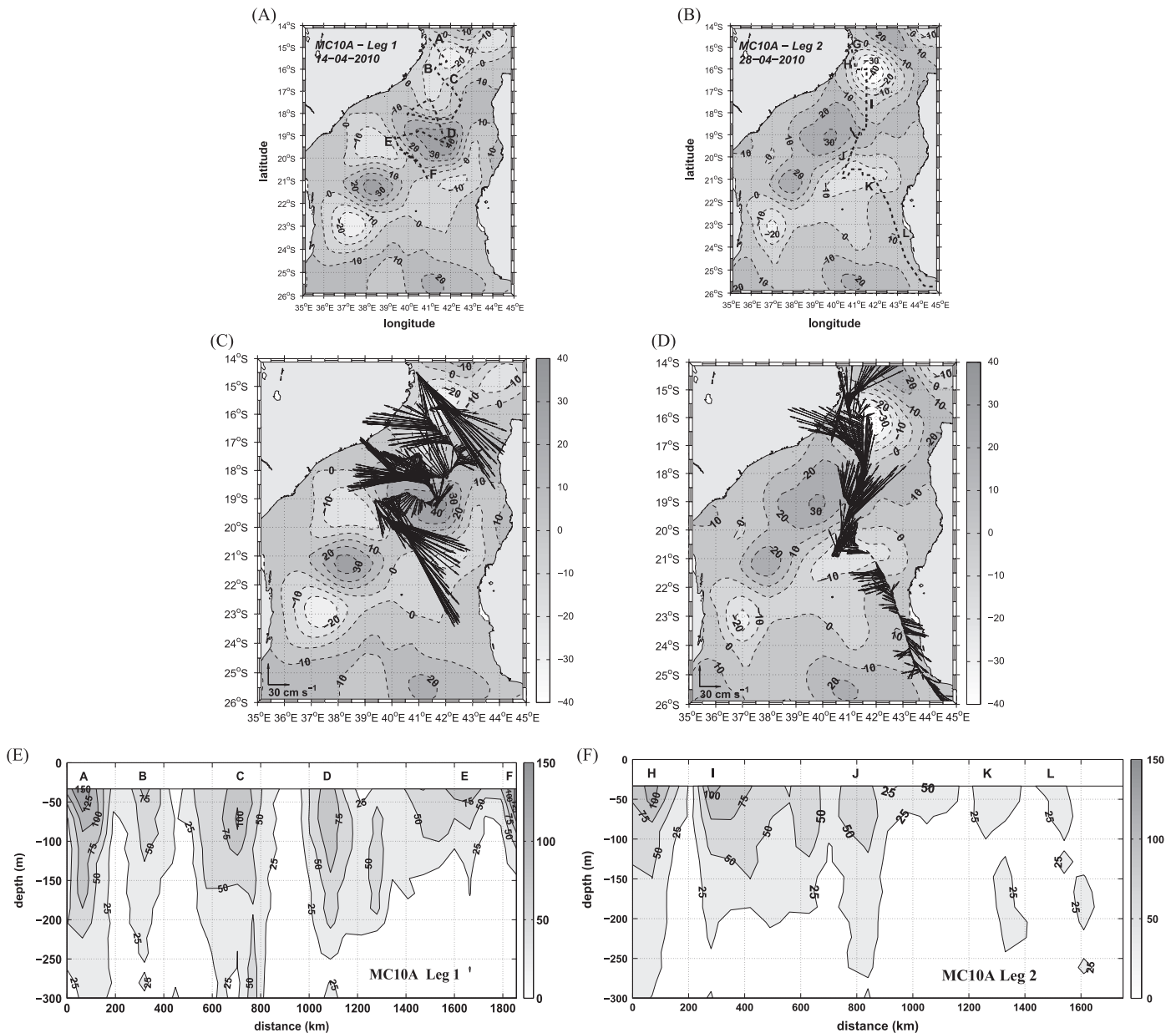
Fig. 7. S-ADCP measurements measured during cruise MC10A: (A, B) cruise tracks over the eddy field observed on 14 and 28 April 2010, (C, D) surface velocity (0–50 m) over the eddy field, and (E, F) velocity to a depth of 300 m. Grey scale in (A–D) indicates SLA (cm). Grey scale in (E, F) indicates velocity (cm s^{-1}). Velocity scale in (C, D) is shown in the bottom left corner. Note that the strong coastal current at the start of leg 2 (G) is not visible in (D) as this section is plotted off the continental shelf (see also Fig. 8).

between altimetry and drifters (Kelly et al., 1998; Lagerloef et al., 1999; Ducet et al., 2000) and between altimetry and current metre moorings (Menkes et al., 1996; Ducet et al., 2000). In the tropical Pacific, Menkes et al. (1996) mentioned a bias (rms difference) of 0.14 m s^{-1} between in situ and altimetry derived velocities, while Lagerloef et al. (1999) found biases of 0.1 m s^{-1} in the west and 0.3–0.4 m s^{-1} in the east from current metre measurements. In the MZC, Swart et al. (2010) found that velocity derived from altimetry was underestimated by about 0.2 m s^{-1} when compared to drifters deployed within an anticyclone.

3.4.2. Surface drifter trajectories and SLA comparison

In a complementary paper by Hancke et al. (2014), the surface circulation in the MZC has been investigated using 67 satellite drifters released in the MZC since 2003. Despite good general agreement between surface velocities derived from the drifter

trajectories and those for the gridded geostrophic currents, some differences are noticeable. An example is shown in Fig. 10 where velocity and direction of both current estimates are compared along a 5.5 month drifter track. Remarkable features are the presence of sporadic peaks in the magnitude of drifter velocity (Fig. 10B), as well as differences in the direction of the currents (Fig. 10A, C). This corroborates the hypothesis of an a-geostrophic, wind driven component of the surface circulation in the MZC. The comparison between the daily mean surface currents estimated from the full drifter data set and the geostrophic current derived from altimetry indicates that the geostrophic velocities are lower than those of the drifters (not shown).

3.5. Wind component of the circulation in the MZC

Comparison between the Ekman surface currents derived from the daily 1/2° wind (QuikSCAT scatterometer) and the
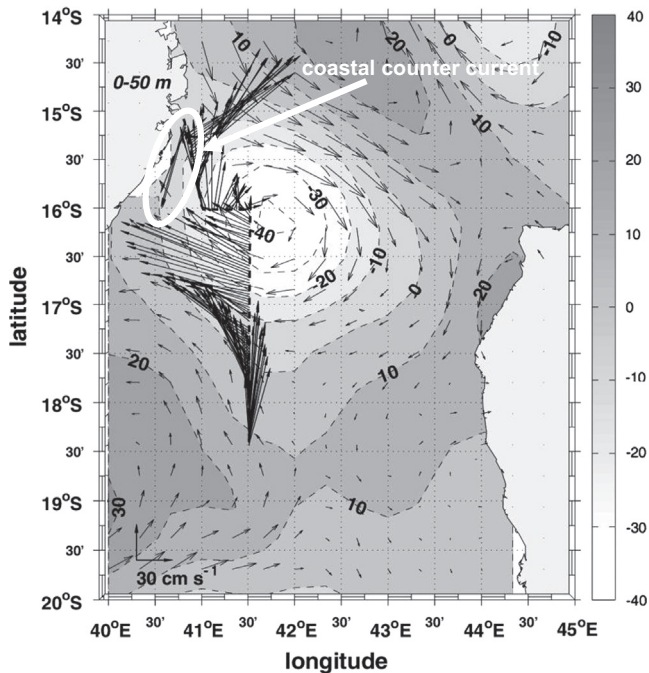
Fig. 8. Near surface (0–50 m) velocity distribution over the eddy field for 14 April 2010 during leg 2 of cruise MC10A. Grey scale indicates SLA (cm). Velocity scale is shown in the bottom left corner. The surface geostrophic velocity from altimetry (not scaled) is superimposed on the SLA map. Note the thin coastal counter current close to the shelf.

altimetry-derived geostrophic currents for the time series from 2003 to 2009 shows that in most cases the geostrophic component is at least one order of magnitude higher (not shown). In some instances, however, strong wind events are observed to drive an Ekman surface current of the same order of magnitude in a different direction. Such an event was noted by Hancke et al. (2014) when a surface drifter was moved out of an anticyclone into an adjacent cyclone when crossing the trajectory of a tropical, atmospheric cyclone with wind > 30 m s^{-1}. Other occurrences of a drifter shift between adjacent eddies were reported under lighter wind conditions (Hancke et al., 2014). This illustrates the potential of wind driven surface circulation in the MZC to drive the transport of passive (including biological) material close to the surface even in a context of ubiquitous mesoscale features.

The analysis of satellite wind velocity (2003–2010 time series) highlighted the occurrence of strong wind events in each zone of the $4° \times 4°$ gridded area defined for the MZC (Table 2, Fig. 11A). For each zone, the percentage of wind speed within velocity ranges was calculated on a yearly base and averaged over the full time series (Fig. 11). Low to medium (0–4 and 4–8 m s^{-1}) velocities were dominant over the whole MZC except in the two southeast zones (9 and 10) in the vicinity of Madagascar. Wind velocities in the range 8–12 m s^{-1} (corresponding to surface Ekman velocities of 0.15–0.25 m s^{-1}) occurred at frequencies of 10–15% in the zones north of 20°S (1–4) and 20–40% to the south of this latitude (zones 5–10). The faster wind velocity class (12–16 m s^{-1}, corresponding to Ekman velocities of 0.25–0.35 m s^{-1}) represented only 1% of the occurrences north of 20°S, 3.5% of the occurrences between 20° and 24°S (zones 5–6) and up to 9% in the southeast MZC (zones 9–10). Only a few wind events occurred in the 16–20 m s^{-1} class, corresponding probably to the passage of atmospheric cyclones in the area. The same analysis on a seasonal basis (monsoon cycle, not shown) confirmed the lower velocities north of 20°S during the period of northeast monsoon (November–February) but did not show significant changes in the southern MZC. Interestingly,

the highest winds occurred south of 20°S and east of 40°E where the mesoscale eddy dynamics was less developed and geostrophic currents were weaker (zones 6, 9, 10). This analysis demonstrated and quantified the potential of wind driven circulation to exceed the geostrophic component in specific circumstances.

4. Discussion

4.1. Dipole history and eddy traceability

The generation processes of anticyclones in the Channel narrows at ~16°S have been described from satellite observations (Schouten et al., 2003), *in situ* measurements with the mooring line deployed at 16°S (Harlander et al., 2009; Ridderinkhof et al., 2010) and numerical models (Backeberg and Reason, 2010; Halo et al., 2014). Harlander et al. (2009) clearly showed the different steps leading to the formation of an anticyclonic cell (their Fig. 7), which is triggered by strong southward flow in the east of the Channel narrows. Using a high resolution regional circulation model, Backeberg and Reason (2010) showed that this process is connected to the transport variability of the SEC north of Madagascar. Positive (anticyclonic) vorticity is generated at the inshore edge of the SEC as it flows westward past the northern tip of Madagascar and propagates into the northern basin of the MZC where eventually an anticyclonic eddy is formed. Such scenarios correspond with the "classical" scheme (or normal situation) of eddy formation in the MZC, resulting in the propagation of anticyclones along the western side of the MZC (e.g. Schouten et al., 2003). This was presumably the situation for most of the cruises in this study (April 2005, September 2007, December 2008 and April 2010).

From a statistical analysis of sea level height (SSH), Palastanga et al. (2006) highlighted the intermittent presence of positive SSH anomalies in the eastern MZC. During our study, anticyclones in the central part of the channel were shown to increase in strength when they merged with these positive anomalies, as already suggested by Schouten et al. (2003). This was clearly the case in April 2005 and in April 2010. In December 2008, there was no positive SSH anomaly near the west coast of Madagascar, but an isolated anticyclone formed in the east during September and subsequently merged with a southwesterly moving anticyclonic structure. In contrast, no contribution from the east to the eddy migrating southward in the western basin was evident in September 2007 and November 2009.

While the formation of anticyclones at the Channel narrows is the most common and most effective process, the analysis of SLA confirmed that areas of anticyclonic eddy generation exist elsewhere in the Channel. As mentioned above, anticylones might originate from positive SSH anomalies periodically observed in the eastern MZC. Alternatively, anticyclones formed at the southern tip of Madagascar may enter the Channel from the south and merge with other anticyclonic eddies propagating southwards. These different generation sites are in agreement with the results of Halo et al. (2014) who used high resolution regional circulation models to show that a variety of eddy (both cyclonic and anticyclonic) generation sites exist within the Channel.

The complex history of anticyclonic cells makes it difficult to infer biogeochemical properties related to the eddy dynamics. In particular, the concept of "constrained" versus "free" eddies used by Bakun (2006) to express reversed biological signatures of an eddy depending on its maturation is valid in an open ocean but seems questionable for the MZC. Eddy–eddy (or eddy–shelf) interactions add complexity to the evolution of particular eddies. This was observed in 2010 where an anticyclone shifted from the centre of the Channel to the western boundary within a few days. Such behaviour complicates the analysis of the eddy driven biological response.

(A)

(B)
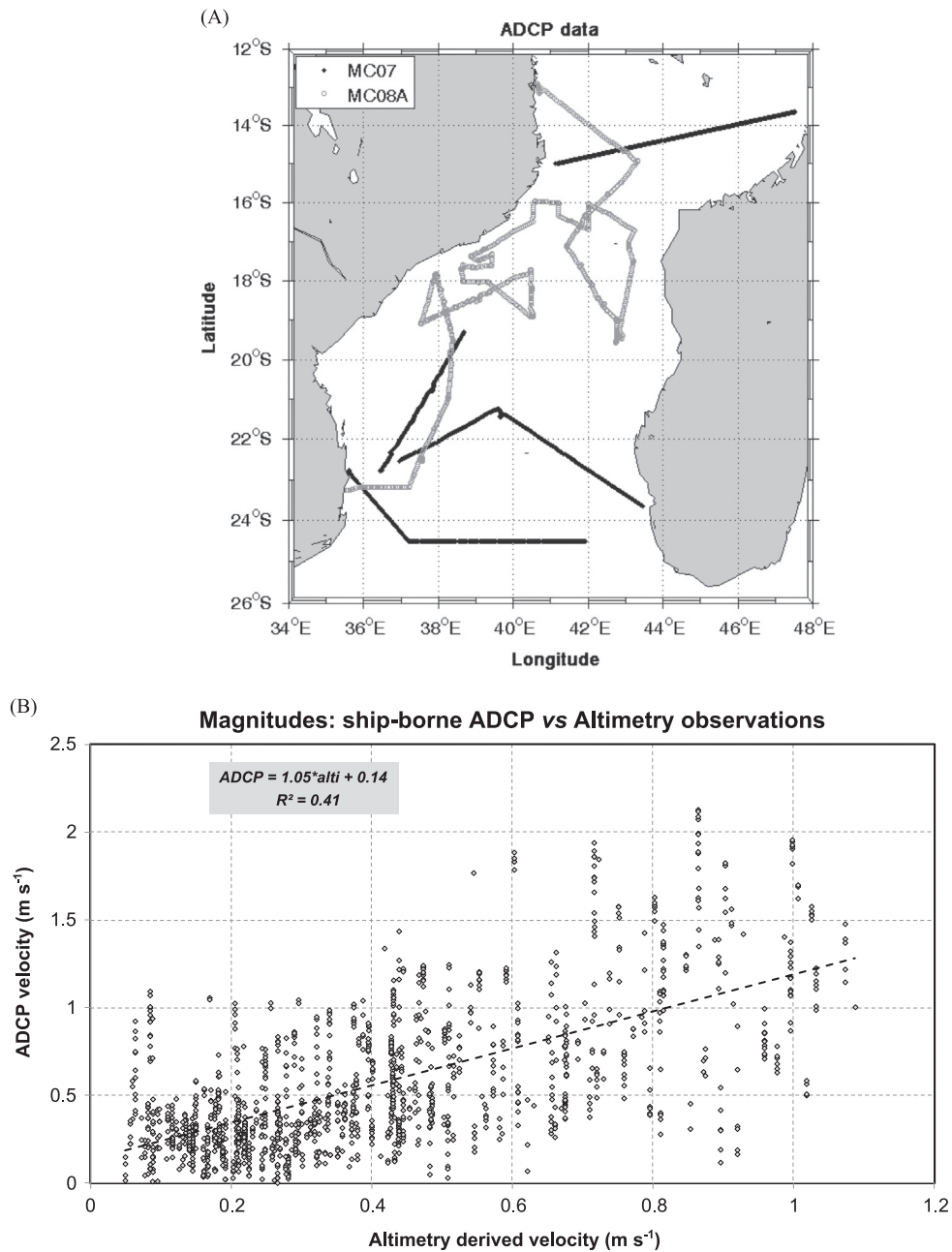
Fig. 9. Comparison of S-ADCP surface (0–50 m) velocity for the 2007 and 2008 cruises and geostrophic velocity derived from altimetry for the corresponding date and location: (A) ship tracks used for the comparison, (B) regression between altimetry-derived and ADCP measured velocities. The linear model, with uncertainties on the coefficients, is presented. The vertical line effect of the dot distribution is due to the nearest neighbour procedure used to interpolate geostrophic velocity ($\Delta x=33$ km) to the ADCP position ($\Delta x=5$ km).

4.2. Cyclonic component of the eddy field

There is no documented process that describes the generation of cyclonic eddies in the MZC, except at some particular locations where such structures appear to be (semi) permanent (lee eddies) (Lutjeharms and Jorge da Silva, 1988; Lutjeharms, 2006). SLA time series show that cyclones in the MZC are constrained by the evolution of the anticyclonic eddy field. The signature of cyclonic eddies, however, was clearly evident in in situ measurements of the horizontal current distribution, the vertical structure of isopycnals, the vertical distribution of nutrients, and biogeochemical signatures such as the deep chlorophyll maxima (Lamont et al., 2014; Roberts et al., 2014). These features appear to be closely linked to the dynamics of anticyclonic eddies.

In some circumstances, however, cyclones remain stable over several weeks and do so independently from the dominant anticyclonic eddy field. This was the case in April 2010 when a cyclone remained near the narrows (14°–17°S) from mid-March to mid-May. This particular eddy had dynamical characteristics comparable to the anticyclones that generally form at the narrows and migrate southward in the west of the channel. Such a fully developed structure may well influence local ecosystems through upwelling, transport and shelf interaction. For comparison, eddy characteristics of this cyclone (Fig. 7) and the cyclone–anticyclone pair investigated at 18°S in 2008 (Fig. 6) are presented in Table 3. The cyclone in 2008 is considered representative of the cyclonic eddies in the MZC.

A stable cyclonic structure has been observed repeatedly in the SLA time series data on the eastern side of the Comoran Basin.

(A)

(B)

Velocity Magnitude (cm s^{-1}) : Mean difference (drifter minus aviso) = 10 cm s^{-1}

(C)

Direction (degrees) : Mean difference (drifter minus aviso) = −14°

01/10/2007−10/03/2008
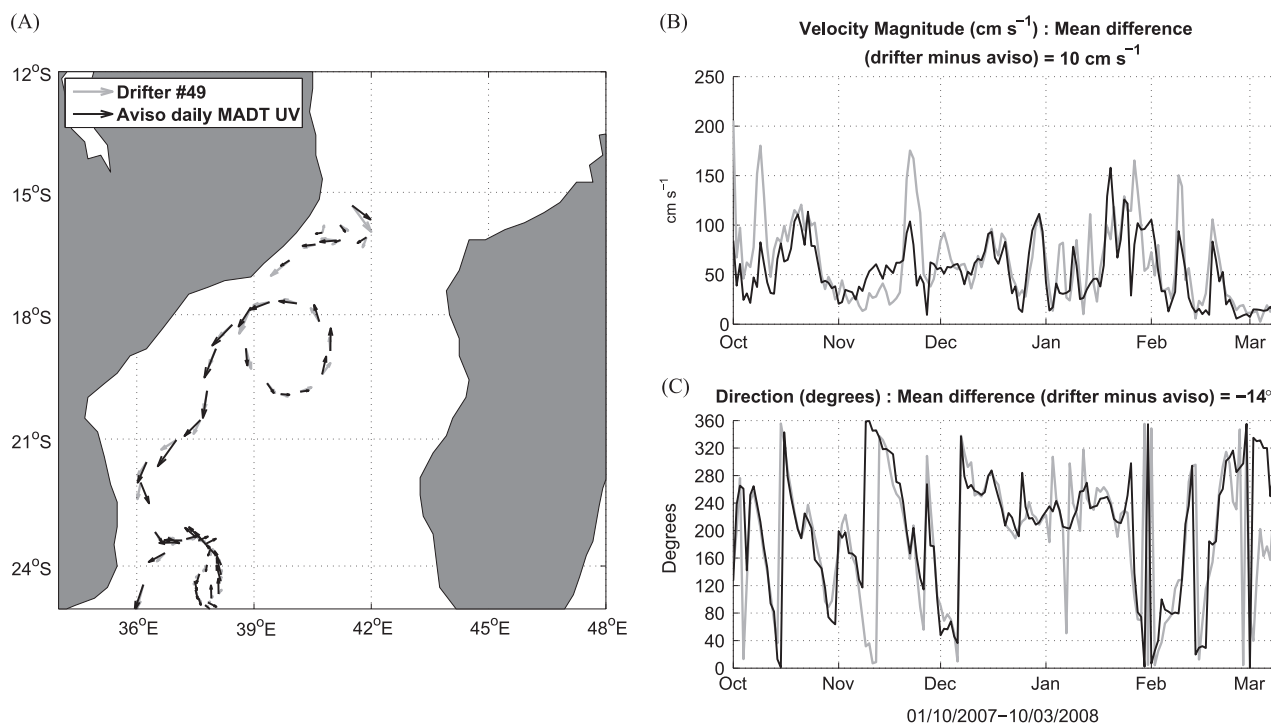
Fig. 10. Comparison of a surface drifter (number 49, 1 October 2007–2010 March 2008) and geostrophic velocity derived from altimetry for the corresponding date and location: (A) drifter track in the MZC, (B) drifter (light grey) and geostrophic (black) velocity along the drifter track, and (C) drifter (light grey) and geostrophic (black) velocity direction along the drifter track.

Such a cyclone was investigated (S-ADCP) in September 2007 (Fig. 2B). A similar cell was also observed in October 2008 that shifted westward and extended across the Channel narrows between 14° and 16°S and was sampled a few weeks later at the beginning of the 2008 cruise. The presence of a cyclonic eddy in the northeast of the MZC seems to be a common feature of the circulation in the northern MZC, even if not observed on a regular basis. For instance, no occurrence was apparent in the DT weekly SSH maps in 1997, but 16 and 26 occurrences were found in 1996 and 1998 respectively. There is no clear signature on the mean eddy field (e.g. Schouten et al., 2003) but cyclonic eddies have been reported at these locations by Donguy and Piton, (1991), De Ruijter et al. (2002) and Pripp et al. (2014). This eddy is superimposed on the general anticyclonic circulation in the northern MZC (Backeberg and Reason, 2010). Northeast cyclones were not present during the two periods of January–April 2005 and March–May 2010 where eddy formation was associated with the presence of a positive SSH anomaly in the eastern MZC.

4.3. Circulation in the southeastern MZC

The relatively invariable sea surface topography in the southeast MZC compared to the mesoscale eddy field over most of the Channel does not seem to hinder substantial currents in this area. This was evident from S-ADCP current measurements in September 2007 east of the transect at 24.5°S (Fig. 3) and in April 2010 along the coast of Madagascar. Southeasterly (2007) and easterly (2010) currents were measured in the surface layer that were apparently not related to any strong eddy structures. A thin coastal current was evident along Madagascar in 2007 at 23.5°–24°S, which was clearly disconnected from the wider flow in the same direction ~100 km away from the coast. The flow consisted of a current core of about 20 km width and 200 m depth with maximum speed at the surface of ~50 cm s^{-1} (the current in 2010 was weaker, ~25 cm s^{-1} at the surface, L in Fig. 7D). Measurements during the cruises do not indicate the origin of these coastal flows

as the current data were not corrected for tides, and we cannot rule out a tidal component of a few cm s^{-1} in this area.

The gridded wind data (QuickSCAT in 2007, ASCAT in 2010) showed moderate southeasterlies at the time of the measurements, indicating that these currents cannot be driven by the wind. Interestingly, southeasterly flow along the southwestern coast of Madagascar was proposed in earlier circulation schemes in the MZC (Fig. 1A in Saerte and Jorge da Silva, 1984; Donguy and Piton, 1991). The presence of cyclonic eddies, potentially formed in the lee of the southern tip of Madagascar (Cap Sainte Marie), is evident in SeaWiFS chlorophyll composite images (Quartly and Srokosz, 2004). Surface drifters also clearly showed the occurrence of southeasterly coastal currents along Madagascar (Hancke et al., 2014). The east and southeast regions are not as well studied as the rest of the MZC and observations during the MESOBIO cruises highlighted the complexity of the circulation in this area. Moreover, the potential effect of coastal currents on the living resources available to the Madagascar population makes it essential to obtain a better understanding of the circulation in this part of the MZC.

4.4. Altimetry versus in situ observations of the eddy field.

The description of the eddy field within the MZC has mainly been based on altimetry observation (e.g. Schouten et al., 2003). The mooring line deployed in the Channel narrows confirmed eddy formation and their southward migration at this latitude (e.g. Ridderinkhof and De Ruijter, 2003; Harlander et al., 2009; Ridderinkhof et al., 2010). Observations along transects perpendicular to the coast of Mozambique at 20°S and 24°S (Swart et al., 2010) also indicated anticyclonic eddy activity along the coast of Mozambique. In the present study, the substantial in situ current data set obtained between 2005 and 2010 has been used to test the accuracy of the geostrophic approximation for the MZC. While the geostrophic currents (from altimetry) and in situ measurements (S-ADCP and drifters trajectories) clearly showed good
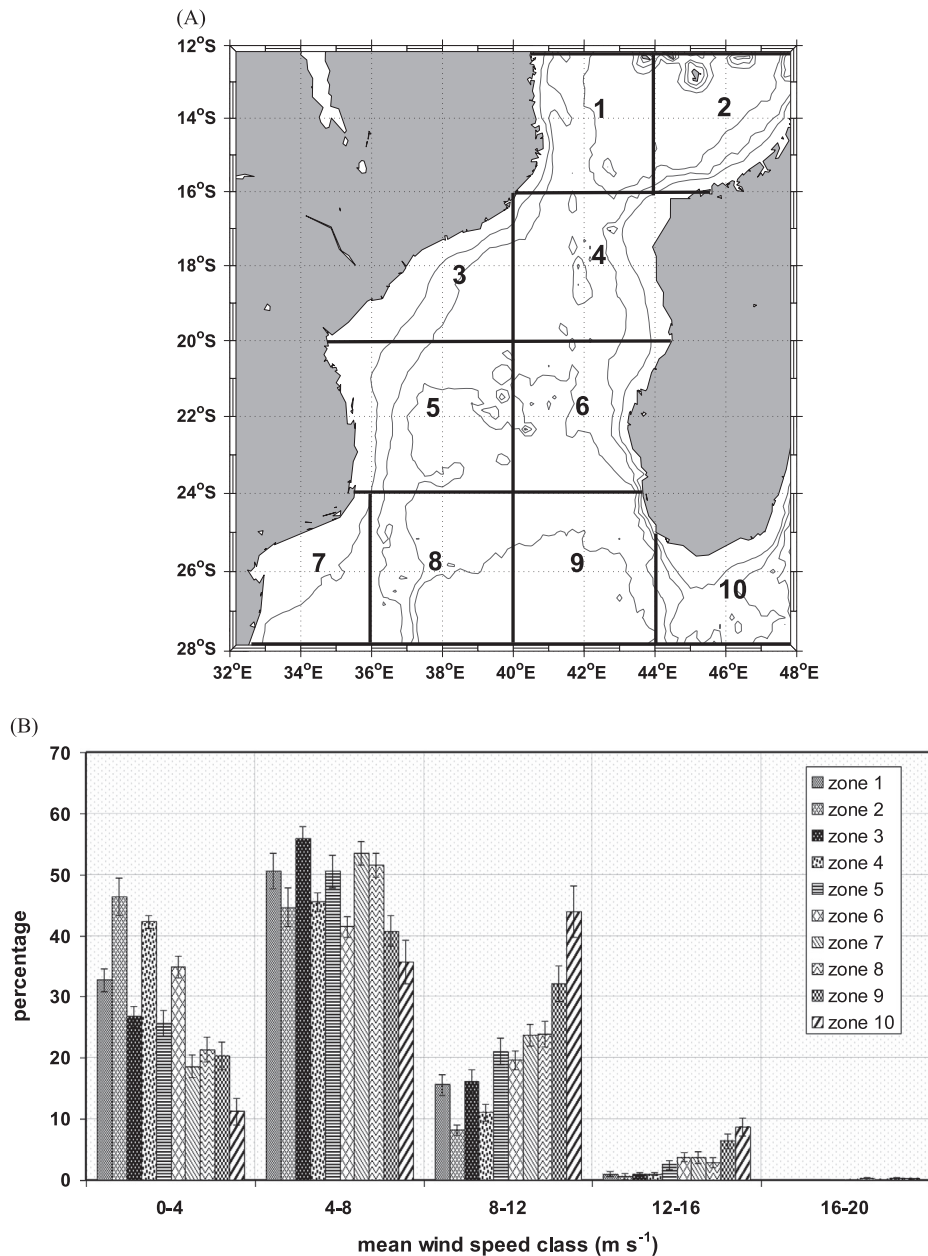
Fig. 11. (A) Zonal division of the Mozambique Channel for wind analysis. (B) Histogram of the mean wind speed for each zone and speed class, averaged for a year over the period 2003–2010. Error bars represent the standard deviation of the mean for the 8 years of satellite data.

Table 3

Mean characteristics of the cyclone sampled at 16°S in April 2010 and the cyclone–anticyclone pair sampled at 18°S in December 2008. Vertical extension is the maximum depth of the 50 cm s^{-1} contour (cyclone 2010 and anticyclone 2008) and 25 cm s^{-1} contour (cyclone 2008).

	Maximum SLA (cm)	Edge velocity (cm s^{-1})	Vertical extension (m)
Cyclone at 16°S (2010)	−40	125	200
Anticyclone at 18°S (2008)	30	175	250
Cyclone at 18°S (2008)	−15	< 50	100

qualitative agreement, altimetry based currents were underestimated compared to in situ measurements. Departures of the drifter trajectories from altimetry-derived geostrophic currents

also occurred on several occasion (Hancke et al., 2014), even apart from the occurrence of high wind events (see below).

The underestimate of velocity deduced from altimetry was already observed by Swart et al. (2010). The first reason is the very different spatial and temporal resolution of each type of measurement, where a resolution of 1/3° and 1 day for the altimetry is compared to the instantaneous and localised S-ADCP measurements and daily averaged data from drifters. A further limitation is that the S-ADCP acquires data at 8 m while the surface drifters are drogued at 15 m. It should be noted that the geostrophic velocity field deduced from altimetry has been significantly improved by the use of multi-mission altimetry products (Ducet et al., 2000) and of the Rio09 Mean Dynamic Topography recently released, which includes an improved estimate of the geoid (Rio et al., 2011). Despite these improvements, the velocity field remains smoothed and underestimated compared with the in situ measurements. Using data from moorings across the Channel narrows,

Ridderinkhof et al. (2010) determined that high frequency variability may be significant relative to lower frequency geostrophic dynamics, which is not captured by altimetry and could thus contribute to the underestimate of velocity by altimetry.

A second reason is that an a-geostrophic component of the velocity field was expected. An Ekman component of the surface circulation was evident in the drifter trajectories in the case of strong wind events (Hancke et al., 2014), although the global data set we used did not allow an estimate of a systematic bias resulting from the wind. However, regarding the independence of the eddy field and the wind distribution, and that geostrophic currents are weak in the centre of an eddy, moderate winds might drive significant Ekman surface drift relative to the eddy induced velocity in these particular circumstances. This may have a significant influence on the transport of drifting organisms but short time variability in the wind field makes it difficult to quantify the wind effect. A-geostrophic currents were also evident in coastal currents measured at 16°S off Mozambique in April 2010 and at 23.5°S off Madagascar in September 2007. While most of the previous studies on the circulation in the MZC focussed on the mesoscale eddy component and the modulation by large scale variability, a-geostrophic currents need to be considered, particularly for understanding connectivity in the MZC ecosystem.

5. Summary and conclusion

Recent in situ measurements have been presented to illustrate eddy features and processes occurring in the MZC. The observations not only confirmed the presence of eddies and dipoles in the MZC but also documented the horizontal and vertical flow characteristics in and around these structures. Tracking has confirmed that eddies preferentially form in the northern MZC and then migrate southwestward along the western boundary of the Channel. Anticyclones were generally the dominant structure within the eddy field, and current signatures were evident to depths of 500 m for anticyclones and to 100 m for cyclones. In the most common situation, cyclones appeared to be "by-products" of anticyclonic mesoscale dynamics, as already described (e.g. de Ruijter et al., 2002), and tend to be weaker.

An alternative unusual scenario was also observed in our study, however, whereby a dominant cyclonic feature developed in the narrows of the MZC (e.g. April 2010). The characteristics of this cyclone (sea surface elevation, speed at its edge, depth penetration) were comparable to that of anticyclones generally present at this latitude (Table 3). Due to their pronounced dynamical signature, these cyclonic structures may have a local impact on biological productivity. The presence of a cyclonic cell in the northeastern MZC basin also seems to be a common feature that is superimposed on the general anticyclonic circulation in the northern basin. The development of the cell into a strong eddy feature, as in April 2010, might be linked to the presence of positive SLA in the eastern Channel as already mentioned by Palastanga et al. (2006), resulting in an alternative, and temporary, mesoscale scenario in the MZC. In the situation surveyed in April 2010, a very narrow coastal current flowing in an opposite direction to the western edge current of the cyclone was observed. Our measurements do not allow us to conclude whether such currents are typically associated with cyclones located in the narrows, nor if these might be part of the episodic continuous Mozambique Channel Current as recently described by Lutjeharms et al. (2012).

The a-geostrophic component (i.e. not driven by mesoscale turbulence) of the MZC circulation has been shown to be significant at times. Wind may play a important role during extreme weather conditions, such as atmospheric cyclones that occur almost every year within the MZC. Also, the circulation southeast

of Madagascar appears to be independent of mesoscale activity at times, and should be investigated more directly in future studies.

The mesoscale dynamics observed using in situ measurements during the MESOBIO cruises has implications for the biological productivity within MZC ecosystems. Due to the interactions between the eddies themselves, the interactions with the shelf as well as the influence of inter-annual variability linked to large scale remote forcing such as the El Niño Southern Oscillation and the Indian Ocean Dipole, the variability at a local scale is high and mostly unpredictable. To better understand local processes, including connectivity and biodiversity issues, investigations over long time periods need to be undertaken, taking into consideration the role that regional and basin scale variability may have on the ecosystems.

References

Backeberg, B.C., Reason, C., 2010. A connection between the South Equatorial Current north of Madagascar and Mozambique Channel eddies. Geophys. Res. Lett. 37, L04604.

Bakun, A., 2006. Fronts and eddies as key structures in the habitat of marine fish larvae: opportunitiy, adaptative response and competitive advantage. Sci. Mar. 70, 105–122.

Beal, L.M., De Ruijter, W.P.M., Biastoch, A., Zahn, R., SCOR/WCRP/IAPSO Working Group 139, 2011. On the role of the Agulhas system in ocean circulation and climate. Nature 472, 429–436.

Biastoch, A., Krauss, W., 1999. The role of mesoscale eddies in the source regions of the Agulhas Current. J. Phys. Oceanogr. 29, 2303–2317.

Biastoch, A., Reason, C.J.C., Lutjeharms, J.R.E., Boebel, O., 1999. The importance of flow in the Mozambique Channel to seasonality in the greater Agulhas Current system. Geophys. Res. Lett. 26, 3321–3324.

Bigg, G.R., 1992. Validation of trends in the surface wind field over the Mozambique Channel. Int. J. Climatol. 12, 829–838.

Chapman, P., Di Marco, S.F., Davis, R.E., Coward, A.C., 2003. Flow at intermediate depths around Madagascar based on ALACE float trajectories. Deep-Sea Res. II 50, 1957–1986.

Da Silva, J.C.B, New, A.L., Magalhaes, J.M., 2009. Internal solitary waves in the Mozambique Channel: observations and interpretation. J. Geophys. Res. 114, C05001.

Davison, A.C., Hinkley, D.V., 1997. Bootstrap Methods and Their Application. Cambridge University Press, Cambridge.

De Ruijter, W.P.M., Ridderinkhof, H., Lutjeharms, J.R.E., Schouten, M.W., Veth, C., 2002. Observations of the flow in the Mozambique Channel. Geophys. Res. Lett. 29, 1502.

De Ruijter, W.M.P., van Aken, H.M., Beier, E.J., Lutjeharms, J.R.E., Matano, R.P., Schouten, W.M., 2004. Eddies and dipoles around South Madagascar: formation, pathways and large-scale impact. Deep-Sea Res. I 51, 383–400.

De Ruijter, W.P.M., Brummer, G.-J.A., Drijfhout, S.S., Lutjeharms, J.R.E, Peeters, F., Ridderinkhof, H., Van Aken, H., Van Leeuwen, P.J., 2006. Observations of the inter-ocean exchange around South Africa. EOS Trans. AGU 87, 97–101.

Di Marco, S.F., Chapman, P., Nowlin Jr., W.D., Hacker, P., Donohue, K., Luther, M., Johnson, G.C., Toole, J., 2002. Volume transport and propery distributions of the Mozambique Channel. Deep-Sea Res. II 49, 1481–1511.

Donguy, J.-R., Piton, B., 1991. The Mozambique Channel revisited. Oceanol. Acta 14, 549–558.

Ducet, N., Le Traon, P.-Y., Reverdin, G., 2000. Global high-resolution mapping of ocean circulation from TOPEX/Poseidon and ERS-1 and -2. J. Geophys. Res. 115 (C8), 19477–19498.

Gründlingh, M.L., 1989. Two contra-rotating eddies of the Mozambique Ridge Current. Deep-Sea Res. 36, 149–153.

Halo, I., Backeberg, B., Penven, P., Ansorge, I., Reason, C., Ulgren, J., 2014. Eddy properties in the Mozambique Channel: A comparison between observations and two numerical ocean circulation models. Deep-Sea Res. II 100, 38–53.

Hancke, L., Roberts, M.J., Terrnon, J.F., 2014. Characteristics of the surface circulation in the Mozambique Channel from satellite-tracked drifters. Deep-Sea Res. II 100, 27–37.

Harlander, U., Ridderinkhof, H., Schouten, M.W., De Ruijter, W.P.M., 2009. Long-term observations of transport, eddies, and Rossby waves in the Mozambique Channel. J. Geophys. Res. 114, C02003.

Harris, T.W.F., 1972. Sources of the Agulhas Current in the spring of 1964. Deep-Sea Res 19, 633–650.

Kelly, K.A., Beardsley, R.C., Limeburner, R., Brink, K.H., Paduan, J.D., Chereskin, T.K., 1998. Variability of the near-surface eddy kinetic energy in the California Current based on altimetric, drifter, and moored current data. J. Geophys. Res. 103 (C6), 13067–13083.

Lagerloef, G.S.E., Mitchum, G.T., Lukas, R.B., Niller, P., 1999. Tropical Pacific near-surface currents estimated from altimeter, wind, and drifter data. J. Geophys. Res. 104 (C10), 23313–23326.

Lamont, T., Barlow, R.G., Morris, T., van den Berg, M.A., 2014. Characterization of mesoscale features and phytoplankton variability in the Mozambique Channel. Deep-Sea Res. II 100, 94–105.

Le Traon, P.-Y., Dibarboure, G., 1999. Mesoscale mapping capabilities of multi-satellite altimeter missions. J. Atmos. Oceanic Technol 16, 1208–1223.

Lutjeharms, J.R.E., Jorge da Silva, A., 1988. The Delagoa Bight eddy. Deep-Sea Res. 35, 619–634.

Lutjeharms, J.R.E., Wedepohl, P.M., Meeuwis, J.M., 2000. On the surface drift of the East Madagascar and Mozambique Currents. S. Afr. J. Sci. 96, 141–147.

Lutjeharms, J.R.E., 2006. The coastal oceans of south-eastern Africa. In: Robinson, A.R., Brink, K.H. (Eds.), The Sea, vol. 14. John Wiley, NewYork, pp. 781–832.

Lutjeharms, J.R.E., Biastoch, A., van der Werf, P.A., Ridderinkhof, H., de Ruijter, W.P.M., 2012. On the discontinuous nature of the Mozambique Current. S. Afr. J. Sci. 108 http://dx.doi.org/10.4102/sajs.v108i1/2.428.

Malauene, B.S., Shillington, F.A., Roberts, M.J., Moloney, C.L., 2014. Cool, elevated-chlorophyll waters off northern Mozambique. Deep-Sea Res. II 100, 68–78.

Manders, A.M.M., Maas, L.M.R., Gerkema, T., 2004. Observations of internal waves in the Mozambique Channel. J. Geophys. Res. 109, C12034.

Menkes, C., Boulanger, J.-P., Busalacchi, A.J., 1996. Evaluation of TOPEX and basin-wide Tropical Ocean and Global Atmosphere-Tropical Atmosphere Ocean sea surface topographies and derived geostrophic currents. J. Geophys. Res 100 (C2), 25087–25099.

Murat Yilmaz, H., 2007. The effect of interpolation methods in surface definition: an experimental study. Earth Surf. Process. Landforms 32, 1346–1361.

Niiler, P.P., Sybrandy, A.S., Bi, K., Poulain, P.M., Bitterman, D., 1995. Measurements of water-following capability of holey-sock and TRISTAR drifters. Deep-Sea Res. 42, 1951–1964.

Palastanga, V., van Leeuwen, P.J., de Ruijter, W.P.M., 2006. A link between low-frequency mesoscale eddy variability around Madagascar and the large-scale Indian Ocean variability. J. Geophys. Res. 111, C09029.

Pascual, A., Faugère, Y., Larnicol, G., Le Traon, P.-Y., 2006. Improved description of the ocean mesoscale variability by combining four satellite altimeters. Geophys. Res. Lett. 33, L02611.

Penven, P., Lutjeharms, J.R.E., Florenchie, P., 2006. Madagascar: a pacemaker for the Agulhas Current system? Geophys. Res. Lett. 110, C10021.

Pond, S., Pickard, G.L., 1983. Introductory Dynamical Oceanography, second ed. Pergamon Press, Oxford.

Pripp, T., Krakstad, J.O., Mortensen, P.B., Gammelsrød, T., 2014. Physical influence on the biological production along the western shelf of Madagascar. Deep-Sea Res. II 100, 174–183.

Quartly, G.D., Srokosz, M.A., 2004. Eddies in the southern Mozambique Channel. Deep-Sea Res. II 51, 69–83.

Rio, M.H., Guinehut, S., Larnicol, G., 2011. The new CNES-CLS09 global mean dynamic topography computed from the combination of GRACE data, altimetry and in-situ measurements. J. Geophys. Res. 116, C07018.

Ridderinkhof, H., De Ruijter, W.P.M., 2003. Moored current observations in the Mozambique Channel. Deep-Sea Res. II 50, 1933–1955.

Ridderinkhof, H., Van der Werf, P.M., Ullgren, J.E., Van Aken, H.M., Van Leeuwen, P.J., De Ruijter, W.P.M., 2010. Seasonal and interannual variability in the Mozambique Channel from moored current observations. J. Geophys. Res. 115, C06010.

Roberts, M.J., Ternon, J.F., Morris, T., 2014. The mesoscale eddy field in the Mozambique Channel in December 2008. Deep-Sea Res. II 100, 54–67.

Saerte, R., Jorge da Silva, A., 1984. The circulation of the Mozambique Channel. Deep-Sea Res. 31, 485–508.

Saerte, R., 1985. Surface currents in the Mozambique Channel. Deep-Sea Res. 32, 1457–1467.

Saji, N.H., Goswami, B.M., Vinayanchandran, P.N., 1999. A dipole mode in the tropical Indian Ocean. Nature 401, 360–363.

Sete C., Ruby, J., Dove, V., 2002. Seasonal variation of tides, currents, salinity and temperature along the coast of Mozambique. ⟨http://hdl.handle.net/1834/188⟩. Instituto Nacional de Hidrografia e Navigaçâo, Maputo.

Schouten, M.W., De Ruijter, W.P.M., Van Leeuwen, P.J., Ridderinkhof, H., 2003. Eddies and variability in the Mozambique Channel. Deep-Sea Res. II 50, 1987–2003.

Stewart, R.H., 2004. Introduction to physical oceanography. Department of Ocea-nography, Texas A&M University, ⟨http://oceanworld.tamu.edu/resources/ocng_textbook/contents.html⟩, 355pp.

Swart, N.C., Lutjeharms, J.R.E., Ridderinkhof, H., de Ruijter, W.P.M., 2010. Observed characteristics of Mozambique Channel eddies. J. Geophys. Res. 115, C09006.

Thomson, R.E., LeBlond, P.H., Rabinovich, A.B., 1998. Satellite tracked drifter measurement of inertial and semidiurnal currents in the northeast Pacific. J. Geophys. Res. 103 (C1), 1039–1052.

Uchida, H., Imawaki, S., Hu, J.-H., 1998. Comparison of Kuroshio surface velocities derived from satellite altimeter and drifting buoy data. J. Oceanogr. 54, 115–122.